

A. Abdibekova , D. Zhakebayev , A. Zhumali

Al-Farabi Kazakh National University, Almaty, Kazakhstan,
e-mail: Dauren.Zhakebaev@kaznu.kz,

Stuart number effect on 3-d mhd convection in a cubic area

Abstract. In this paper mathematical modeling of magnetohydrodynamics natural convection in three dimensional area at different Stuart numbers has been considered. The magnetic field is considered vertically and results have been shown at different planes of 3-D enclosure. The modeling of natural convection is based on the solution of a filtered unsteady three - dimensional Navier- Stokes equation and the equation for temperature. The problem is solved numerically: the equations of motion and temperature – by a finite-difference method in combination with penta-diagonal matrix using the Adams-Bashfort scheme, the equation for pressure – by spectral Fourier method with combination of matrix factorization. Change the dynamic of natural convection is gained over the time depending on the different values of Stuart numbers. As result of modelling, isothermal surfaces, velocity and temperature contours, also profiles for different Stuart numbers are obtained.

Key words. Natural convection, magnetohydrodynamics, finite difference method, spectral method.

Introduction

Natural convection is a phenomenon that occurs in many engineering applications, resulting in airflow near surfaces of solid particles or liquids, such as airflow in double-glazed windows, airflow in double-glazed doors of refrigerated display cases and airflow in gaps or cavities building walls. To clearly understand, many researchers have devoted themselves to the study of this phenomenon in order to enhance or reduce this heat transfer mode. Natural convection of the flow is one of the most important problems in fluid mechanics and [1,2].

Magnetic field convection has been developed and has been used in recent decades [3-7]. In [8], two-dimensional mixed convection in a chamber was solved using the finite volume method. They examined the sinusoidal boundary condition and the effect of the ratio of amplitudes, phase deviation, Richardson number and Hartmann number on the heat transfer rate. Their results show that the Nusselt number increases in amplitude ratio. In addition, the Nusselt number increases with the phase deviation to $\varphi = \pi/2$, and then decreases. In [9], the results for a laminar mixed convection flow in the presence of a magnetic field in the upper cavity controlled by a cover with a set of Grashof and Hartmann numbers are presented. They used the finite volume method to model the equations and concluded that

the transfer rate decreases with the Hartmann number.

In [10], the Boltzmann MRT double lattice method was applied to simulate three-dimensional MHD of natural convection flow in a cubic cavity. Two different populations with models D3Q19 and D3Q7 were used to determine the flow field and temperature, respectively. The effect of the Hartmann and Grashof numbers on the projection of the flow trace and the heat transfer rate on various surfaces of the cavity, where the flow structure and isotherms in different planes of the casing change sharply due to an increase in the Hartmann and Grashof numbers, since the magnetic field is strong, the rates are suppressed.

Three-dimensional nanofluidic non-Darsian natural convection is presented in the presence of Lorentz forces [11]. The lattice Boltzmann method is selected for mesoscopic analysis. The simulation results are presented for various amounts of Darcy, Rayleigh, and Hartmann numbers, and the volume fraction of Al₂O₃. The results show that convection dominates at large Darcy and Rayleigh numbers; therefore, distorted isotherms are observed at high Darcy and Rayleigh numbers. The motion of the nanofluid increases with increasing volume fraction, the Rayleigh and Darcy numbers, but decreases with increasing Hartmann number. The temperature gradient on a hot surface decreases with increasing

Hartmann number, while it increases with increasing Darcy number, Rayleigh number. The influence of the use of nanoparticles reaches a maximum degree for the maximum Hartmann value and the minimum value of the Darcy and Rayleigh numbers.

In [12], convective flows and heat transfer in a magnetic field were studied. They also use the finite volume method and report that the heat transfer rate is increasing. In [13], the LBM method was used to solve a two-dimensional MHD flow in an inclined cavity with four heat sources. They thought that the double model of multiple time relaxation models the equations of momentum and energy, and explores the effect of the Hartmann number on fluid flow and heat transfer. They show that the average Nusselt number decreases due to an increase in the Hartmann number for all Rayleigh numbers.

In [14], MHD natural convection in a three-dimensional square cavity with a sinusoidal temperature distribution on one side wall was investigated using the new Boltzmann lattice method with a double relaxation time model using nano-liquid copper-water. The influence of various parameters, such as the Rayleigh and Hartmann numbers, the volume fraction of nanoparticles, and the phase deviation on heat transfer, was considered. Concerning the present results, the following conclusions are drawn: Convection heat transfer decreases with increasing Hartmann number, and the average Nusselt number decreases for both the left and right walls, but the decrease for the right wall is greater than for the left. When the Hartmann number increases from 0 to 50, the average Nusselt

number decreases by 64% and 70% for the left and right walls, respectively.

In this paper, we consider a mathematical model of the problem of natural convection under the influence of a vertical magnetic field, where the effect of the Stuart number on convection of the MHD flow was obtained.

The applied magnetic field $B = -H_0 \vec{j}$ effect in the Navier-Stokes equations is the inclusion of the Lorentz force to the momentum equations $F_l = J \times B$, where $J = \sigma(E + V \times B)$ - is electric current density, E - is electric field strength, which we set equal to zero, and σ is electric conductivity, $V = u_1 \vec{i} + u_2 \vec{j} + u_3 \vec{k}$ velocity of fluid, and all of these in combination we obtain $F_l = \sigma(V \times B) \times B$ - Lorentz force, where $F_l = \sigma[(u_1 \vec{i} + u_2 \vec{j} + u_3 \vec{k}) \times (-H_0 \vec{j})] \times (-H_0 \vec{j})$ is in detail, after using the properties of the multiplication of unit vectors, we obtain $F_l = \sigma(u_1 H_0 \vec{k} - u_3 H_0 \vec{i}) \times (-H_0 \vec{j})$, or $F_l = \sigma(-u_1 H_0^2 \vec{i} - u_3 H_0^2 \vec{k})$, and $F_l = F_1 + F_2 + F_3$, where $F_1 = -\sigma u_1 H_0^2$, $F_2 = 0$, $F_3 = -\sigma u_3 H_0^2$.

The problem is based on solving non-stationary equations of magnetohydrodynamics with filtration in combination with the continuity equation, equations for temperature, equations of motion of charged particles, taking into account the continuity equation in a Cartesian coordinate system in dimensionless form

$$\begin{cases} \frac{\partial \bar{u}_i}{\partial t} + \frac{\partial(\bar{u}_i \bar{u}_j)}{\partial x_j} = -\frac{\partial \bar{p}}{\partial x_i} + \frac{1}{\text{Re}} \frac{\partial}{\partial x_j} \left(\frac{\partial \bar{u}_i}{\partial x_j} \right) + F_i + \frac{Ra}{\text{Re}^2 \text{Pr}} \bar{\theta}, \\ \frac{\partial \bar{u}_i}{\partial x_i} = 0, \\ \frac{\partial \bar{\theta}}{\partial t} + \frac{\partial(\bar{u}_i \bar{\theta})}{\partial x_j} = \frac{1}{\text{Re Pr}} \frac{\partial}{\partial x_j} \left(\frac{\partial \bar{\theta}}{\partial x_j} \right), \end{cases} \quad (1)$$

where \bar{u}_i ($i = 1, 2, 3$) are the velocity components, $\bar{F}_1 = -N\bar{u}_1$, $\bar{F}_2 = 0$, $\bar{F}_3 = -N\bar{u}_3$ - non-dimensional Lorentz force [10], $N = \frac{\sigma L H_0^2}{\rho \nu_0} = \frac{Ha^2}{\text{Re}}$ is the

Stuart number, where $Ha = H_0 L \sqrt{\sigma / \mu}$ - Hartmann number, H - magnetic field strength, σ is the conductivity of the medium, which is determined from plasma physics.

$U_0 = \sqrt{\alpha D(T_1 - T_0)L_3}$ – characteristically velocity,
 \bar{p} is the full pressure, t is the time,
 $\bar{\theta} = (T - T_0)/(T_1 - T_0)$ – non-dimensional
 temperature in ionosphere, where T_0 and T_1 are
 the respective temperatures of the minimum and
 maximum of the area, $Ra = \frac{\alpha g(T_1 - T_0)L_3^3}{\nu D}$

-Rayleigh, where α is volumetric thermal
 expansion coefficient, g – acceleration due to

gravity, $Re = \sqrt{\frac{Ra}{Pr}}$ is the Reynolds number,

$Pr = \frac{\nu}{D}$ – Prandtl number, D – diffusion
 coefficient, L is the typical length, ν is the
 kinematic viscosity coefficient, ρ is the density of
 the flow.

A schematic picture of the computational
 domain is shown in Figure 1, where the left wall -
 indicated by the blue color, corresponds to the low
 temperature of flow. The right wall layer -
 highlighted in red, corresponds to high temperature
 of the flow.

Initial conditions for temperature, velocity
 components are set zero in all directions of the

domain. The boundary conditions imposed for
 temperature is Dirichlet on the right and left
 boundary, and Neumann on the other directions of
 the domain. The velocity components are equal to 0
 in all directions.

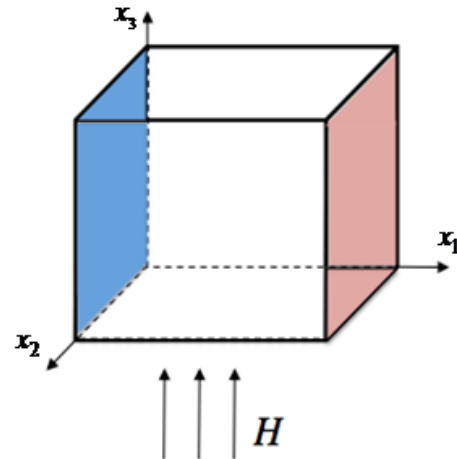


Figure 1 – Illustration of the problem statement

Numerical method

To solve the problem of homogeneous
 incompressible MHD turbulence, a scheme of
 splitting by physical parameters is used:

$$\begin{aligned} \text{I. } & \frac{(\bar{u}^*)^{n+1} - (\bar{u})^n}{\Delta t} - \frac{1}{2Re} \nabla^2 (\bar{u}^*)^{n+1} = \frac{1}{2Re} \nabla^2 (\bar{u})^n + \frac{3}{2} K^n - \frac{1}{2} K^{n-1}, \\ \text{II. } & \Delta p = \frac{\nabla(\bar{u}^*)^{n+1}}{\tau}, \\ \text{III. } & \frac{(\bar{u})^{n+1} - (\bar{u}^*)^{n+1}}{\Delta t} = -\nabla p, \\ \text{IV. } & \frac{\bar{\theta}^{n+1} - \bar{\theta}^n}{\Delta t} - \frac{1}{2Pe} \nabla^2 \bar{\theta}^{n+1} = \frac{1}{2Pe} \nabla^2 \bar{\theta}^n + \left(\frac{3}{2} G^n - \frac{1}{2} G^{n-1} \right) \end{aligned}$$

where

$$K^n = -(\bar{u}^n \nabla) \bar{u}^n + F^n + \frac{Ra}{Re^2 Pr} \theta^n,$$

$G^n = -(\bar{u}^n \nabla) \theta^n$ where $Pe = Re Pr$ – Peclet
 number.

During the first stage, the full magneto
 hydrodynamic equation system is solved without
 the pressure consideration. For approximation of the

convective and diffusion terms of the intermediate
 velocity field a finite-difference method in
 combination with penta-diagonal matrix is
 used, which allowed to increase the order of
 accuracy in space. The numerical algorithm for the
 solution of incompressible MHD turbulence is
 considered at [15].

At the second step, the pressure Poisson
 equation is solved, which ensures that the continuity

equation is satisfied. The Poisson equation is transformed from the physical space into the spectral space by using a Fourier transform. To solve the three-dimensional Poisson equation, the spectral conversion in combination with matrix sweeping algorithm is developed [15]. The resulting pressure field in the third stage is used to recalculate the final velocity field [16].

At the fourth stage, the equation for temperature is solved by using Adams-Bashforth scheme.

Consider the temperature distribution in the horizontal direction at the point i, j, k :

$$\begin{aligned} \frac{\partial \theta}{\partial t} + \frac{\partial(u_1\theta)}{\partial x_1} + \frac{\partial(u_2\theta)}{\partial x_2} + \frac{\partial(u_3\theta)}{\partial x_3} &= \\ &= \frac{1}{\text{Re Pr}} \left(\frac{\partial^2 \theta}{\partial x_1^2} + \frac{\partial^2 \theta}{\partial x_2^2} + \frac{\partial^2 \theta}{\partial x_3^2} \right) \end{aligned} \quad (2)$$

When using the explicit Adams-Bashfort scheme for convective terms and the implicit Crank-Nicholson scheme for viscous terms, equation (2) takes the form:

$$\begin{aligned} \theta_{i,j,k}^{n+1} - \theta_{i,j,k}^n &= -\frac{3\Delta t}{2} [hr]_{i,j,k}^n + \\ &+ \frac{\Delta t}{2} [hr]_{i,j,k}^{n-1} + \frac{\Delta t}{2} [ar]_{i,j,k}^n + \frac{\Delta t}{2} \cdot \frac{1}{\text{Re Pr}} \times (3) \\ &\times \left[\left(\frac{\partial^2 \theta}{\partial x_1^2} \right)_{i,j,k}^{n+1} + \left(\frac{\partial^2 \theta}{\partial x_2^2} \right)_{i,j,k}^{n+1} + \left(\frac{\partial^2 \theta}{\partial x_3^2} \right)_{i,j,k}^{n+1} \right] \end{aligned}$$

where

$$\begin{aligned} [hr]_{i,j,k}^n &= \left(\frac{\partial(u_1\theta)}{\partial x_1} \right)_{i,j,k}^{n+1} + \\ &+ \left(\frac{\partial(u_2\theta)}{\partial x_2} \right)_{i,j,k}^{n+1} + \left(\frac{\partial(u_3\theta)}{\partial x_3} \right)_{i,j,k}^{n+1} \\ [ar]_{i+\frac{1}{2},j,k}^n &= \frac{1}{\text{Re Pr}} \times \\ &\times \left[\left(\frac{\partial^2 \theta}{\partial x_1^2} \right)_{i,j,k}^n + \left(\frac{\partial^2 \theta}{\partial x_2^2} \right)_{i,j,k}^n + \left(\frac{\partial^2 \theta}{\partial x_3^2} \right)_{i,j,k}^n \right] \end{aligned}$$

Discretization of convective expressions looks like this:

$$\left(\frac{\partial u_1 \theta}{\partial x_1} \right)_{i,j,k} = \frac{-(u_1 \theta)_{i+2,j,k} + 27(u_1 \theta)_{i+1,j,k} - 27(u_1 \theta)_{i,j,k} + (u_1 \theta)_{i-1,j,k}}{24\Delta x_1} + O(\Delta x_1^4),$$

$$\left(\frac{\partial u_2 \theta}{\partial x_2} \right)_{i,j,k} = \frac{(u_2 \theta)_{i+1,j-2,k} - 27(u_2 \theta)_{i,j-1,k} + 27(u_2 \theta)_{i,j,k} - (u_2 \theta)_{i,j+1,k}}{24\Delta x_2} + O(\Delta x_2^4)$$

$$\left(\frac{\partial u_3 \theta}{\partial x_3} \right)_{i,j,k} = \frac{(u_3 \theta)_{i,j,k-2} - 27(u_3 \theta)_{i,j,k-1} + 27(u_3 \theta)_{i,j,k} - (u_3 \theta)_{i,j,k+1}}{24\Delta x_3} + O(\Delta x_3^4).$$

Discretization of diffusion conditions looks like this:

$$\left(\frac{\partial^2 \theta}{\partial x_1^2} \right)_{i,j,k} = \frac{-(\theta)_{i+2,j,k} + 16 \cdot (\theta)_{i+1,j,k} - 30 \cdot (\theta)_{i,j,k} + 16 \cdot (\theta)_{i-1,j,k} - (\theta)_{i-2,j,k}}{12\Delta x_1^2},$$

$$\left(\frac{\partial^2 \theta}{\partial x_2^2} \right)_{i,j+\frac{1}{2},k} = \frac{-(\theta)_{i,j+2,k} + 16 \cdot (\theta)_{i,j+1,k} - 30 \cdot (\theta)_{i,j,k} + 16 \cdot (\theta)_{i,j-1,k} - (\theta)_{i,j-2,k}}{12\Delta x_2^2},$$

$$\left(\frac{\partial^2 \theta}{\partial x_3^2}\right)_{i,j,k+\frac{1}{2}} = \frac{-\theta_{i,j,k+2} + 16 \cdot \theta_{i,j,k+1} - 30 \cdot \theta_{i,j,k} + 16 \cdot \theta_{i,j,k-1} - \theta_{i,j,k-2}}{12\Delta x_3^2},$$

where

$$(u_1 \theta)_{i,j,k} = \left(\frac{-u_{1i+1,j,k} + 9u_{1i,j,k} + 9u_{1i-1,j,k} - u_{1i-2,j,k}}{16}\right) \cdot \left(\frac{-\theta_{i+1,j,k} + 9\theta_{i,j,k} + 9\theta_{i-1,j,k} - \theta_{i-2,j,k}}{16}\right);$$

$$(u_2 \theta)_{i,j,k} = \left(\frac{-\theta_{i,j+2,k} + 9\theta_{i,j+1,k} + 9\theta_{i,j,k} - \theta_{i,j-1,k}}{16}\right) \cdot \left(\frac{-u_{2i+2,j,k} + 9u_{2i+1,j,k} + 9u_{2i,j,k} - u_{2i-1,j,k}}{16}\right);$$

$$(u_3 \theta)_{i,j,k} = \left(\frac{-\theta_{i,j,k+2} + 9\theta_{i,j,k+1} + 9\theta_{i,j,k} - \theta_{i-1,j,k-1}}{16}\right) \cdot \left(\frac{-u_{3i+2,j,k} + 9u_{3i+1,j,k} + 9u_{3i,j,k} - u_{3i-1,j,k}}{16}\right);$$

Then the left side of equation (3) is denoted by

$q_{i,j,k}$

$$q_{i,j,k} \equiv \theta_{i+1,j,k}^{n+1} - \theta_{i,j,k}^n \quad (4)$$

From equation (4) we find $\theta_{i,j,k}^{n+1}$

$$\theta_{i,j,k}^{n+1} = q_{i,j,k} + \theta_{i,j,k}^n$$

Replacing all $\theta_{i,j,k}^{n+1}$ from the equations (13), we obtain

$$q_{i,j,k} - \frac{\Delta t}{2} \cdot \frac{1}{\text{Re Pr}} \cdot \left(\frac{\partial^2 q}{\partial x_1^2}\right)_{i,j,k} -$$

$$- \frac{\Delta t}{2} \cdot \frac{1}{\text{Re Pr}} \cdot \left(\frac{\partial^2 q}{\partial x_2^2}\right)_{i,j,k} -$$

$$= \frac{\Delta t}{2} \cdot \frac{1}{\text{Re Pr}} \cdot \left(\frac{\partial^2 q}{\partial x_3^2}\right)_{i,j,k} = -\frac{3\Delta t}{2} [hr]_{i,j,k}^n +$$

$$+ \frac{\Delta t}{2} [hr]_{i,j,k}^{n-1} + \Delta t [ar]_{i,j,k}^n$$

Equation (5) is converted to

$$\left[1 - \frac{\Delta t}{2} \cdot \frac{1}{\text{Re Pr}} \cdot \frac{\partial^2}{\partial x_1^2} - \frac{\Delta t}{2} \cdot \frac{1}{\text{Re Pr}} \cdot \frac{\partial^2}{\partial x_2^2} - \frac{\Delta t}{2} \cdot \frac{1}{\text{Re Pr}} \cdot \frac{\partial^2}{\partial x_3^2}\right] q_{i,j,k} = d_{i,j,k} \quad (6)$$

where

$$d_{i,j,k} = -\frac{3\Delta t}{2} [hr]_{i,j,k}^n + \frac{\Delta t}{2} [hr]_{i,j,k}^{n-1} + \Delta t [ar]_{i,j,k}^n$$

Assuming that equation (6) has second-order accuracy in time, we can instead solve the following equation:

$$\left[1 - \frac{\Delta t}{2} \cdot \frac{1}{\text{Re Pr}} \cdot \frac{\partial^2}{\partial x_1^2}\right] \left[1 - \frac{\Delta t}{2} \cdot \frac{1}{\text{Re Pr}} \cdot \frac{\partial^2}{\partial x_2^2}\right] \left[1 - \frac{\Delta t}{2} \cdot \frac{1}{\text{Re Pr}} \cdot \frac{\partial^2}{\partial x_3^2}\right] q_{i,j,k}^* = d_{i,j,k} \quad (7)$$

We can show that equation (7) is an approximation $O(\Delta t^4)$ to equation (6).

Since the difference between $q_{i,j,k}^*$ and $q_{i,j,k}$ has a higher order, we return to the same notation and just use $q_{i,j,k}$.

To determine $q_{i+\frac{1}{2},j,k}$ the equation (7) is solved in 3 stages:

$$\left[1 - \frac{\Delta t}{2} \cdot \frac{1}{\text{Re Pr}} \cdot \frac{\partial^2}{\partial x_1^2}\right] A_{i,j,k} = d_{i,j,k} \quad (8)$$

$$\left[1 - \frac{\Delta t}{2} \cdot \frac{1}{\text{Re Pr}} \cdot \frac{\partial^2}{\partial x_2^2}\right] B_{i,j,k} = A_{i,j,k} \quad (9)$$

$$\left[1 - \frac{\Delta t}{2} \cdot \frac{1}{\text{Re Pr}} \cdot \frac{\partial^2}{\partial x_3^2}\right] q_{i,j,k} = B_{i,j,k} \quad (10)$$

At the first stage, the $A_{i,j,k}$ search is carried out in the direction of the x_1 coordinates:

$$\left[1 - \frac{\Delta t}{2} \cdot \frac{1}{\text{Re Pr}} \cdot \frac{\partial^2}{\partial x_1^2}\right] A_{i,j,k} = d_{i,j,k}$$

$$A_{i,j,k} - \frac{\Delta t}{2} \cdot \frac{1}{\text{Re Pr}} \cdot \left(\frac{\partial^2 A}{\partial x_1^2}\right)_{i,j,k}^{n+1} = d_{i,j,k}$$

$$A_{i,j,k} - \frac{\Delta t}{2} \cdot \frac{1}{\text{Re Pr}} \cdot \frac{-A_{i+2,j,k} + 16 \cdot A_{i+1,j,k} - 30 \cdot A_{i,j,k} + 16 \cdot A_{i-1,j,k} - A_{i-2,j,k}}{12\Delta x_1^2} = d_{i,j,k}$$

$$s_1 \cdot A_{i+2,j,k} - 16 \cdot s_1 \cdot A_{i+1,j,k} + (1 + 30 \cdot s_1) \cdot A_{i,j,k} - 16 \cdot s_1 \cdot A_{i-1,j,k} + s_1 \cdot A_{i-2,j,k} = d_{i,j,k} \quad (11)$$

where $s_1 = \frac{\Delta t}{24 \cdot \text{Re} \cdot \text{Pr} \cdot \Delta x_1}$.

This equation (11) is solved by the method of the penta-diagonal matrix, which determines $A_{i,j,k}$.

The same procedure is repeated further for directions x_2 in the second stage, namely, $B_{i,j,k}$ is determined by solving equation (9), and the solution from the first stage, as the coefficient on the right, and the s_1 coefficient in the penta-diagonal matrix

are replaced by $s_2 = \frac{\Delta t}{24 \cdot \text{Re} \cdot \text{Pr} \cdot \Delta x_2}$. Finally, in the

third stage, $q_{i,j,k}$ is solved using a similar penta-diagonal system shown in equation (9).

Once we have determined the value $q_{i,j,k}$, we find $\theta_{i,j,k}^{n+1}$

$$\theta_{i,j,k}^{n+1} = q_{i,j,k} + \theta_{i,j,k}^n$$

The other components of temperature θ_{ijk}^{n+1} are solved in a similar way.

Simulation results

The results of modeling the imposition of a vertical magnetic field is obtained, where the lateral distribution of the temperature field is pronounced. The Grashof number is chosen $Gr = 20000$, the Prandtl number $Pr = 0.09$, the Stuart number has the

following values: 1) $N = 0$; 2) $N = 0.09$; 3) $N = 2.16$, kinematic viscosity $\nu = 0.013$ diffusion coefficient equal to $D = 0.14$. For calculations, the mesh size is $34 \times 34 \times 34$. The size of the computational domain is equal to $L_1 = 2\pi$, $L_2 = 2\pi$, $L_3 = 2\pi$, which corresponds to the directions x_1, x_2 and x_3 .

In this paper effect of Stuart number on isothermal surfaces for different Stuart numbers is

shown at Figure 2. It is seen that isothermal surfaces change considerably and gradient of the boundary layer declines with increasing of Stuart number, so heat transfer rate, which depends on the temperature gradient, gradually decreases with increasing magnetic field, which indicates a weakening of the overall heat transfer effect. These trends were also discovered [17–19], who also studied natural convection or Rayleigh Bernard convection under the influence of a magnetic field.

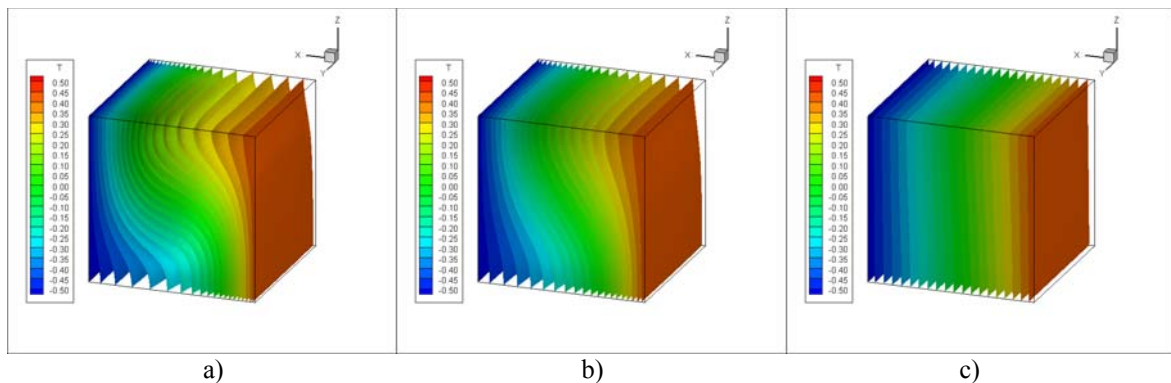


Figure 2 – Isothermal surfaces for various Stuart coefficients
a) $N = 0$; b) $N = 0.09$; c) $N = 2.16$ at $Gr = 20000$

The contours of vertical velocity components, and temperature contours on the different planes of the enclosure are very important for understanding the trend of flow, so present results for the different locations of the cavity have been shown in figures 4 and 5. It is shown at figures 4-5 that, increasing Stuart number isotherm lines become parallel to the walls and temperature gradient on the wall declines, therefore heat transfer rate decreases.

As for the physics of the influence of MHD on the structure of natural convection flows and heat transfer, this is due to the fact that in MHD flows the motion of vortex structures perpendicular to magnetic fields, i.e. horizontally oriented vortex cells, strongly suppressed due to the anisotropic

effect of the magnetic field. This is recognized by the universal effect of magnetic fields, which is theoretically interpreted in [20]. Moreover, another important characteristic of the effect of the vertical magnetic field is that when the magnetic fields are stronger, the vortex structures will be more regular and will be shown parallel to each other.

Consequently, thermal convection caused by the movement of the vortex cells will decrease due to the amplification of magnetic fields.

Figures 6-7 show a longitudinal dimensionless temperature and velocity profile, respectively, for a different number of Stuart 1) $N = 0$; 2) $N = 0.09$ 3) $N = 2.16$. It is observed that the solution has a linear velocity dependence along the transverse direction.

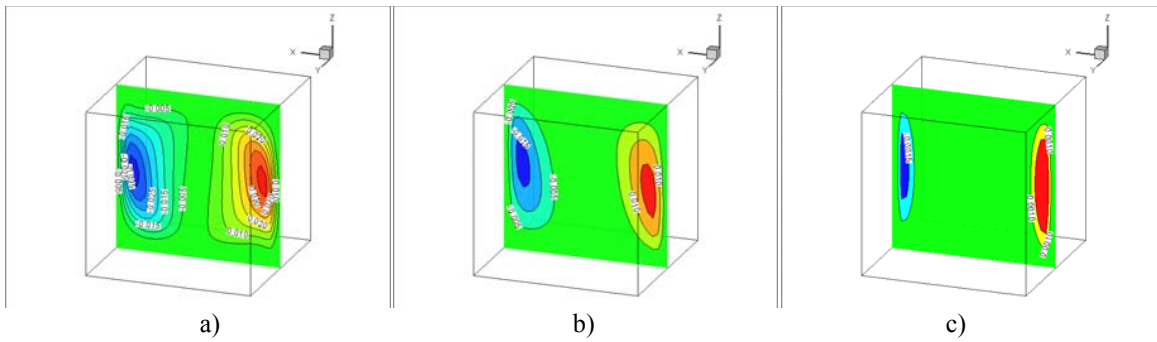


Figure 3 – Contours of x_3 vertical velocity components on $x_2 = 0.5$ plane for different Stuart numbers) $N = 0$; b) $N = 0.09$;c) $N = 2.16$ at $Gr = 20000$

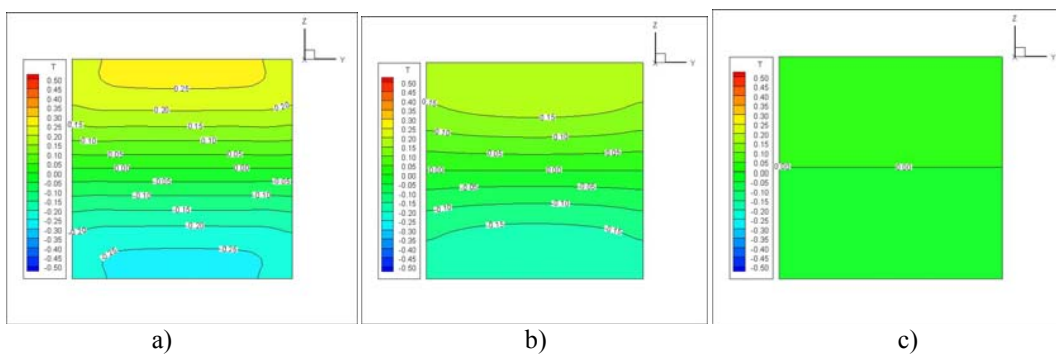


Figure 4 – Temperature contours on $x_1 = 0.5$ plane for different Stuart numbers) $N = 0$; b) $N = 0.09$;c) $N = 2.16$ at $Gr = 20000$

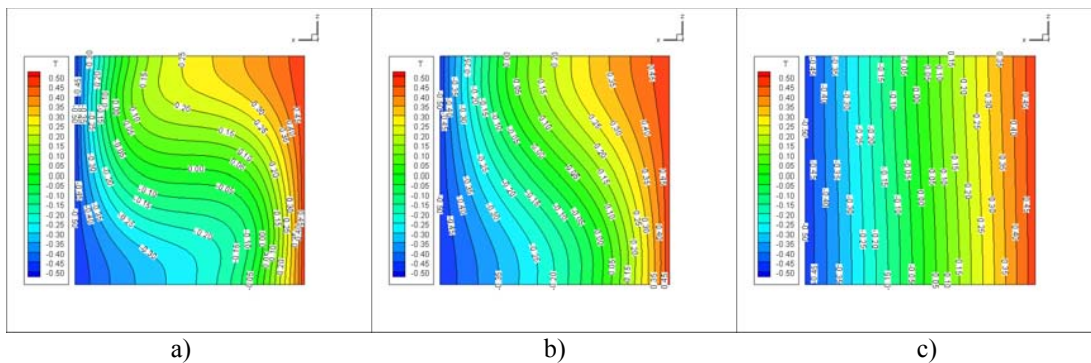


Figure 5 – Temperature contours on $x_2 = 0.5$ plane for different Stuart numbers) $N = 0$; b) $N = 0.09$;c) $N = 2.16$ at $Gr = 20000$

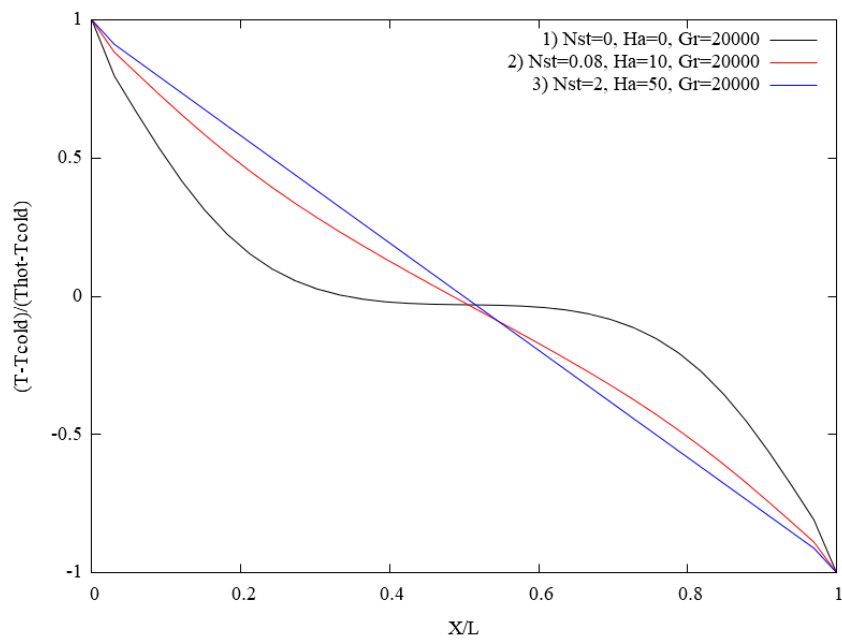


Figure 6 – Temperature profile for different values of the Stuart number
1) $N = 0$; 2) $N = 0.09$; 3) $N = 2.16$ at $Gr = 20000$.

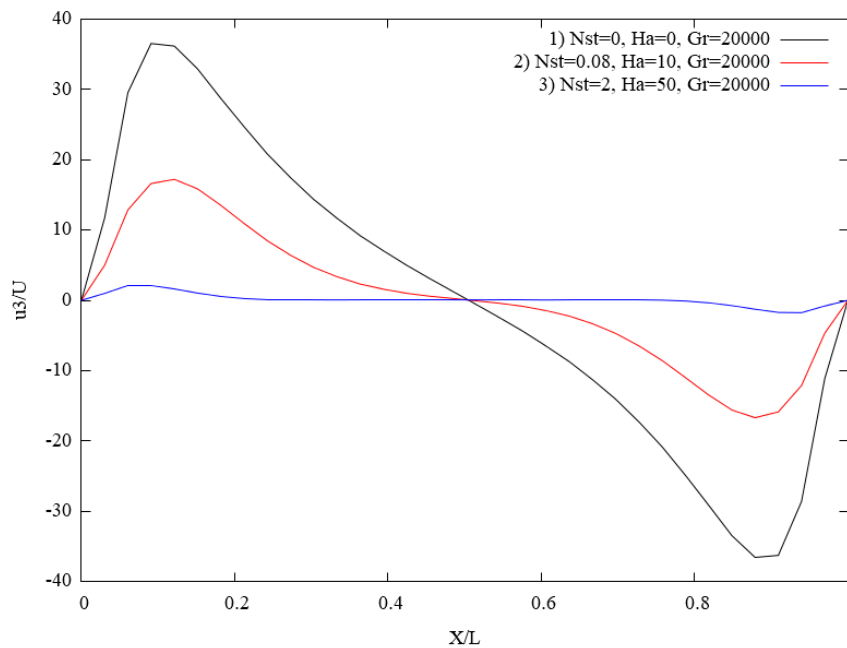


Figure 7 – Velocity profile for different Stuart values
1) $N = 0$; 2) $N = 0.09$; 3) $N = 2.16$ at $Gr = 20000$.

Conclusion

MHD natural convection in a three dimensional area at different Stuart numbers with temperature distribution on side wall has been considered by finite difference method with spectral method.

To solve the equations of flow motion and temperature, the finite difference method is used in combination with a pentadiagonal matrix, and solved by using the Adams-Bashfort scheme. The Poisson equation is solved by spectral method using the fast Fourier transform.

Thus, the following conclusions are drawn: isothermal surfaces change considerably and gradient of the boundary layer declines with increasing of Stuart number, so heat transfer rate, which depends on the temperature gradient, gradually decreases with increasing magnetic field, which indicates a weakening of the overall heat transfer effect. As for the physics of the influence of MHD on the structure of natural convection flows and heat transfer, this is due to the fact that in MHD flows the motion of vortex structures perpendicular to magnetic fields, i.e. horizontally oriented vortex cells, strongly suppressed due to the anisotropic effect of the magnetic field. The effect of the vertical magnetic field is that when the magnetic fields are stronger, the vortex structures will be more regular and will be shown parallel to each other. Consequently, thermal convection caused by the movement of the vortex cells will decrease due to the amplification of magnetic fields.

As result of modelling, isothermal surfaces, velocity and temperature contours, also profiles for different Stuart numbers are obtained.

Acknowledgement

The authors were supported by the Ministry of Education and Science of the Republic of Kazakhstan Grant No. AP05133516.

References

1. Abouei Mehrizi, Farhadi, M., Hassanzadeh Afrouzi, H., Shayamehr, S., Lotfizadeh, H. "Lattice Boltzmann simulation of natural convection flow around a horizontal cylinder located beneath an insulation plate." *J. Theoret. Appl. Mech.* 51(2013): 729–739.
2. Sajjadi, H., Hosseinizadeh, S.F., Gorji, M., Kefayati, Gh.R. "Numerical analysis of turbulent natural convection flow in a square cavity using Large-Eddy Simulation in Lattice Boltzmann." *Iran.J. Sci. Technol., Trans. Mech. Eng.* 35(2011):133–142.
3. Kefayati, G.H.R., Gorji, M., Sajjadi, H., Ganji, D.D. "Lattice Boltzmann simulation of MHD mixed convection in a lid-driven square cavity with linearly heated wall." *Scientia Iranica, Trans. B – Mech. Eng.* 19(2012):1053–1065.
4. Hamid Reza Ashorynejad, Kurosh Sedighi, Mousa Farhadi, Ehsan Fattahi. "Simulating magnetohydrodynamic natural convection flow in a horizontal cylindrical annulus using the lattice Boltzmann method." *Heat Transf. Asian Res.* 41 (2012): 468–483.
5. Ashorynejad, H.R., Abdulmajeed, A., Mohsen Sheikholeslami, M. "Magnetic field effects on natural convection flow of a nanofluid in a horizontal cylindrical annulus using Lattice Boltzmann method." *Int. J. Therm. Sci.* 64(2013):240–250.
6. Xu, B.Q. Li, D.E. Stock. "An experimental study of thermally induced convection of molten gallium in magnetic fields." *Int. J. Heat Mass Transf.* 49(2006): 2009–2019.
7. Grosan, T., Revnic, C., Pop, I., Ingham, D.B. "Magnetic field and internal heat generation effects on the free convection in a rectangular cavity filled with a porous medium." *Int. J. Heat Mass Transfer.* 52(2009):5691–5700.
8. Sivasankaran, S., Malleswaran, A., Lee, J., Sundar, P. "Hydro-magnetic combined convection in a lid-driven cavity with sinusoidal boundary conditions on both sidewalls." *Int. J. Heat Mass Transf.* 54(2011):512–525.
9. Oztop, H.F., Al-Salem, K., Pop, I. "MHD mixed convection in a lid-driven cavity with corner heater." *Int. J. Heat Mass Transf.* 54(2011):3494–3504.
10. Sajjadi, H., Amri Delouei, A., Sheikholeslami, M., Atashafrooz, M., Succi, S. "Simulation of the dimensional MHD natural convection using double MRT Lattice Boltzmann method." *J. Physica A*, 515(2019): 474-496.
11. Sheikholeslami, M. "Lattice Boltzmann method simulation for MHD non-Darcy nanofluid free convection." *J. Physica B*, 516(2017): 55–71.
12. Bhuvaneswari, M., Sivasankaran, S., Kim, Y.J. "Magneto convection in a square enclosure with sinusoidal temperature distributions on both side walls." *Numer. Heat Transf. Part A*, 59(2011):167–184.

13. Zhang, T., Che, D. "Double MRT thermal lattice Boltzmann simulation for MHD natural convection of nanofluids in an inclined cavity with four square heat sources" *Int. J. Heat Mass Transf.* 94(2016): 87–100.
14. Sajjadi, H., Atashafrooz, M. "Double MRT Lattice Boltzmann simulation of 3-D MHD natural convection in a cubic cavity with sinusoidal temperature distribution utilizing nanofluid." *Int. J. of Heat and Mass Trans.*, 126(2018): 489-503. <https://doi.org/10.1016/j.ijheatmasstransfer.2018.05.064>
15. Abdibekova, A., Zhakebayev, D., Abdigaliyeva, A., Zhubat, K. "Modeling of turbulence energy decay based on hybrid methods." *J. Engineering Computations*, 35(2018):1965-1977.
16. Zhakebayev, D., Zhumagulov, B., Abdibekova, A. "The decay of MHD turbulence depending on the conductive properties of the environment." *J. Magnetohydrodynamics* 50(2014):121-138.
17. Burr, U., Müller, U. "Rayleigh–Bénard convection in liquid metal layers under the influence of a horizontal magnetic field." *J. Fluid Mech.* 453 (2002):345–369.
18. Barleon, L., Burr, U., Stieglitz, R., Frank, M. "Heat transfer of a MHD flow in a rectangular duct." in: *Proc. of the 3rd Internat. Conf. on Transfer Phenomena in Magnetohydrodynamic and Electroconducting Flows* (1997).
19. Barleon, L., Jochmann, P., Mack, K., Burr, U., Stieglitz, R. "Experimental investigations on the magneto-convective flow in a vertical gap" *Proceedings of 4th PAMIR Conference* (2000):309–314.
20. Davidson P. "Magnetic damping of jets and vortices." *J. Fluid Mech.* 299 (1995):153–186.